ELSEVIER

Coastal Engineering 24 (1995) 275-296

COASTAL ENGINEERING

Numerical and hydraulic model study of wave decay on a shelf beach

K.A. Rakha, J.W. Kamphuis *

Department of Civil Engineering, Queen's University, Kingston, Ont. K7L 3N6, Canada

Received 8 November 1993; accepted after revision 14 July 1994

Abstract

A number of studies on wave dissipation in the surf zone have been conducted over the past three decades. These studies, however, did not include the case of energy dissipation in the vicinity of a seawall. In this paper two wave energy dissipation models (Dally et al., 1984; Battjes and Janssen, 1978) are modified to account for wave reflection. Dally et al.'s (1984) model is also calibrated against hydraulic model tests for irregular waves on a beach consisting of a constant slope followed by a horizontal shelf. The numerical model developed, predicts the H_{rms} wave decay for the tests performed and the effect of reflection was also well simulated.

1. Introduction

In the surf zone, the wave energy transported from deep water dissipates in the process of wave breaking, and is mainly transformed into turbulence energy. Two approaches are commonly used to evaluate the wave properties in the surf zone. The first approach predicts the variation of the wave properties within a wave cycle. The Boussinesq model is an example of such a detailed model (e.g. Schäffer et al., 1993). The second approach calculates for wave properties averaged over a wave period. In most applications, such a model is sufficient. This paper describes such an averaged model. Wave decay in the surf zone can be predicted by solving the wave energy balance equation;

$$\frac{\mathrm{d}(EC_g)}{\mathrm{d}s} = -D \tag{1}$$

* Corresponding author. Queen's University, Department of Civil Engineering, Kingston, Ont. K7L 3N6, Canada, Phone: 613 545-2148, Fax: 613 545-2128.

SSDI 0378-3839(94)00024-7

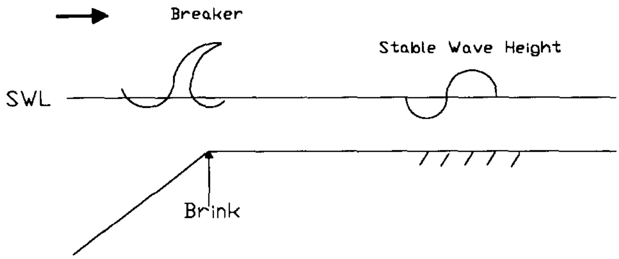

Fig. 1. "Shelf Beach" layout.

where E is the energy density (calculated using linear wave theory), C_g is the group velocity, D is the wave energy dissipation rate per unit area due to breaking, and s is the distance along the wave path.

Integrating Eq. (1) subject to initial conditions, E or the wave height H can be determined as a function of the distance s. However, a formulation for the energy dissipation term D is required to solve the above equation.

Many studies have been undertaken to estimate D over the surf zone. Battjes and Janssen (1978) propose a formulation for D using a bore like model, which was first advanced by LeMéhauté (1962). Dally et al. (1984) suggested an empirical formulation for D which includes energy stabilization. Both these models were developed for cases without wave reflection. In the present study both the above models were modified to account for wave reflection. Dally et al.'s (1984) model was also calibrated for irregular waves on a beach consisting of a uniform slope and a horizontal shelf as shown in Fig. 1. This will be called a "shelf beach" in this paper.

Battjes and Janssen's (1978) model defines wave decay using wave height values obtained from a spectral analysis of the wave record. In the present study, this model which represents total energy is referred to as the Frequency Domain Model (FDM). Dally et al.'s (1984) wave model was developed for the statistical definition of the wave height, obtained from a zero crossing analysis of the time series. The modification of Dally et al.'s individual wave model is thus referred to as a Time Domain Model (TDM). Nairn (1990), and Thompson and Vincent (1984) also distinguished between both the above wave height definitions.

2. Energy dissipation rate

Battjes and Janssen (1978) developed the following equation for D by assuming that all the broken waves have a wave height of H_m,

$$D=\frac{1}{4}fQ\rho gH_m^2 \tag{2}$$

where H_m is the maximum possible wave height in a depth h, f is an average wave frequency and Q is the fraction of waves breaking. The value of Q was obtained by assuming the cumulative probability distribution function (pdf) of all wave heights is of a Rayleigh-type cut off discontinuously at $H = H_m$. This was shown to imply the following relation between Q and (H_{rms}/H_m),

$$\frac{1-Q}{-\ln Q} = \left(\frac{H_{rms}}{H_m}\right)^2 \tag{3}$$

The maximum wave height H_m is determined from a Miche type expression introducing a variable γ, to allow for the influence of wave steepness.

$$H_m = 0.88k^{-1}\tanh\left(\frac{\gamma kh}{0.88}\right) \tag{4}$$

Battjes and Stive (1984) calibrated and verified Battjes and Janssen's dissipation model for random waves. They proposed the use of the peak period of the wave spectrum T_p as the mean period. They also calibrated γ with deep water wave steepness,

$$\gamma = 0.5 + 0.4\tanh\left(\frac{33H_o}{L_{op}}\right) \tag{5}$$

where L_{op} is the deep water wave length calculated using the peak frequency, and H_o is the deep water rms wave height. Nairn (1990) mentioned that the dependency of γ on the wave steepness is opposite to conventional breaker criteria such as Weggel (1972) or Singamsetti and Wind (1982). These criteria (developed for regular waves) suggest that steeper waves break sooner, i.e. with smaller incipient H/d ratios (further offshore). Nairn mentioned that this parameter could be compensating for the shift of energy from incident wave frequencies to long wave motion. Nairn recalibrated the above equation,

$$\gamma = 0.39 + 0.57\tanh\left(\frac{33H_o}{L_{op}}\right) \tag{6}$$

Battjes and Stive (1985) verified that an approximate equation for Q proposed by Thornton and Guza (1983) yields results similar to Eq.(3). The equation proposed by Thornton and Guza relates Q to (H_{rms}/H_m) directly as follows,

$$Q = \left(\frac{H_{rms}}{H_m}\right)^4 \tag{7}$$

Both Eqs. (3) and (7) are plotted in Fig. 2. Although Eq. (7) approximates Eq. (3) closely, the deviation increases for small values of Q. Fig. 2 also shows,

$$\ln Q = 3.86 - 3.86\left(\frac{H_m}{H_{rms}}\right) \tag{8}$$

which is a much closer approximation to Eq. (3). To decrease the computational time and enhance convergence, Eq. (8) was used instead of Eq. (3) for calculating Q in the present model.

Dally et al. (1984) developed a wave energy dissipation model which explicitly takes into account wave height stabilization over a horizontal beach. Dally et al. assumed D in the surf zone to be proportional to the difference between the local energy flux and a stable energy flux,

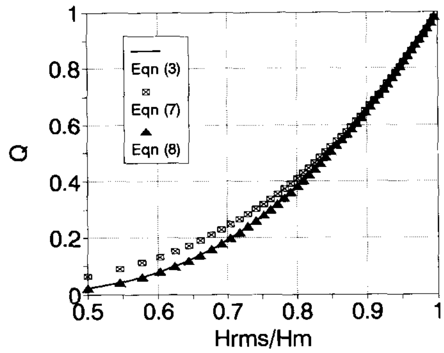

Fig. 2. Different formulations for Q in Eq. (2).

$$D=\frac{K}{h}[(E-E_{st})C_g] \tag{9}$$

where $D \geq 0$, and the local stable wave energy E_{st} is calculated using the stable wave height proposed by Horikawa and Kuo (1966). Horikawa and Kuo (1966) conducted laboratory tests on a shelf beach as shown in Fig. 1. Their data indicated that a stable wave height develops in a water depth h over the horizontal profile. This stable wave condition is attained when no more energy dissipation due to wave breaking occurs. The data published by Horikawa and Kuo (1966) suggest,

$$H_{st}=\Gamma h \tag{10}$$

where Γ is a coefficient which ranges between 0.35 to 0.4.

Dally et al. proposed constant values of $K=0.15$ and $\Gamma=0.4$ to give the best results over a wide range of monotonic beach slopes. These values were recommended for models which included wave setup. If wave setup is not calculated, Dally et al. recommended values of $K=0.17$ and $\Gamma=0.5$. The Dally et al. (1984) model was developed for regular waves only. In a subsequent paper Dally and Dean (1986) developed a model for irregular waves. They divide the offshore wave height distribution into bins, use the joint wave height and period distribution of Longuet-Higgins (1983) and then apply Eqs. (9) and (10) to each bin.

Kamphuis (1994) showed that Eq. (9) may be applied directly to a representative wave height and period. This is similar to Johnson (1990) who used H_{rms} as the representative wave height, and obtained good results. Johnson used a value of $\Gamma_{rms}=0.4$, and suggested a value of $K=0.25$ for the case of wave decay with an opposing current. Recently, Larson (1993) showed that a model for the decay of a single wave parameter (H_{rms}) can produce results very close to a Monte Carlo simulation, such an approach reduces the computational time considerably.

The tests performed by Horikawa and Kuo (1966) were performed, with regular waves, and their results cannot be simply used to calibrate an irregular wave model. Since no detailed study of stable wave heights for irregular waves has been published, irregular wave tests similar to those by Horikawa and Kuo were performed in this study for cases with and without reflection.

3. Modelling of reflection

The wave energy dissipation models described in the previous section deal only with an incident wave. In the vicinity of a seawall reflection off the wall must be included in the wave decay model. It was assumed that only the incident wave dissipates energy through breaking, whereas the reflected wave does not. Jones (1975) made this same assumption together with other approximations to derive an analytical solution for the longshore velocities along a seawall. The tests performed in the present study further showed that the reflected wave does not affect the decay of the incident wave. Thus, the TDM and FDM can be applied simply with the incident wave heights used in Eqs. (8) and (9).

The reflected wave was calculated using a mirror image technique (Carr (1952)). The incident wave heights were determined from a refraction model which marches in the onshore direction. The reflected wave was calculated by marching in the offshore direction starting from the seawall. The details of the wave transformation model and its verification is provided by Rakha and Kamphuis (1994). The total wave height was calculated by summing the energy for the incident and reflected waves,

$$H_t = \sqrt{H_i^2 + H_r^2} \tag{11}$$

where H_t is the total rms wave height, H_i is the incident rms wave height, and H_r is the reflected rms wave height. Goda (1976) mentioned that Eq. (11) is based on two assumptions. The first is that the energy of composite waves appearing as the result of superposition of multiple trains of irregular waves is the sum of the energies of the individual wave trains. The second is that the proportionality of representative wave heights to the square root of wave energy holds for such composite waves too, regardless of the direction of individual wave trains. Goda (1985) also mentioned that this formula is not valid in the immediate vicinity of the seawall because of the fixed phase relation between the incident and reflected waves. Clearly, the above equation can only be applied to a wave height such as the rms and significant wave height defined from the complete wave train, and not for individual wave heights. It will be shown later that the above equation is not valid for H_{max} due to the phase effect. In the present study, it was found that the breaking of the incident wave before reaching the seawall decreases the phase effect.

Over the horizontal section in the wave stabilizing zone shown in Fig. 1 the reflected wave height can be calculated from,

$$H_r = K_r H_i \tag{12}$$

where, K_r is the reflection coefficient. Substituting Eq. (12) into Eq. (11) the following equation for the total wave height is obtained,

$$H_t = \sqrt{1 + K_r^2}\; H_i \tag{13}$$

Silvester (1974) mentioned that K_r is less than unity due to second order effects, where K_r depends on the wave steepness obtained from linear wave theory and the water depth. Goda (1976) showed that the average K_r for a wave spectrum was 0.9 for a 1 : 10 bottom slope and 0.75 for a 1 : 30 bottom slope. In the present study a constant reflection coefficient for the vertical seawall of 0.9 as recommended by Ippen (1966) and Kondo et al. (1986)

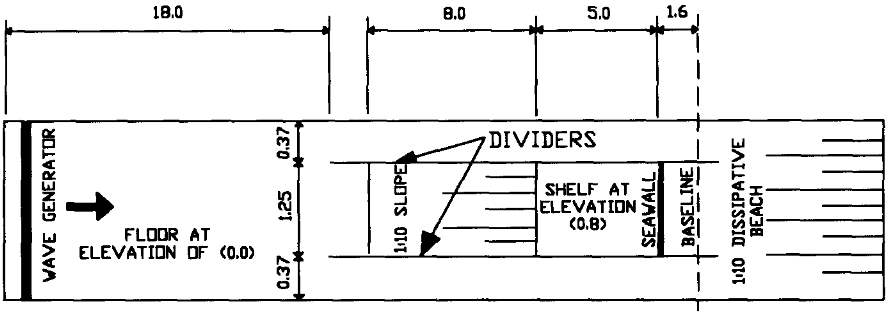

Fig. 3. Plan of 2 m wave flume (dimensions in meters).

was found to yield a good approximation to the wave transformation for the tests performed as shown later.

Smith and Hughes (1993) mentioned that although reflection produced by the structure had a little effect on the non-broken incident wave heights, the breaker location appeared to be affected by the interaction of both waves. They mentioned that the effect of reflection on the breaker location should be studied. For the TDM, the location of the breaker was predicted using the Kamphuis (1991) breaker criterion,

$$H_{sb} = (0.095e^{4.0m})L_{pb}\tanh\left(\frac{2\pi h_b}{L_{pb}}\right) \tag{14}$$

where the subscripts b, p, and s denote breaking, peak frequency of the spectrum, and "significant" respectively. The value of m was calculated as the average slope over one wavelength offshore of the point of interest. For the cases with reflection the total wave height as defined in Eq. (11) was used in Eq. (14). The use of the total wave height in Eq. (14) is validated later in this paper. At breaking H_{sb} was assumed to be equal to $\sqrt{2}H_{rmsb}$. This was shown to be reasonable from earlier work by Briand (1990) and Kamphuis (1991).

4. Laboratory experiments

Tests were performed in the 2 m wide wave flume shown in Fig. 3. The water depth in the flume varied from 0.86 m to 0.98 m. The test section of the flume was 1.25 m wide with 0.37 wide channels at both sides to reduce the secondary reflection off the wave generator. Without the side channels the maximum increase in the incident deep water wave height from secondary reflection would be 30%. The use of the flume layout shown in Fig. 3 resulted in an increase in the incident deep water wave height of only 4–12%. The larger increases occurred for the cases where only a small percentage of the waves broke before reaching the seawall. The beach consisted of a 1 : 10 wooden fixed slope and a 5 m long horizontal section. Fig. 1 shows a vertical cross section of this shelf beach profile. A seawall was constructed at the end of the horizontal section, and dissipative material was placed in front of the seawall to produce the tests without reflection. The seawall was located at a distance of 1.6 m from the baseline.

Table 1
2D tests on a fixed horizontal beach

Name	Type	Depth on shelf (cm)	H_{so} (cm)	T_p (sec)	Number of tests
KA	Irr. + Refl.	6–18	5–9	1.15	17
KA	Irr.	6–18	5–9	1.15	17
KB	Irr. + Refl.	6–18	5–9	1.25	17
KB	Irr.	6–18	5–9	1.25	17
KC	Reg.	6–12	5–13	1.15	13

A total of 68 irregular wave tests were performed both with and without reflection as shown in Table 1. The water depth on the horizontal shelf was varied from 6 to 18 cm in increments of 2 cm. The deep water rms wave heights tested ranged from 3.5 to 7 cm. Two peak wave periods of 1.15 and 1.25 sec were tested. A JONSWAP wave spectrum was used with a groupiness factor of 0.8 and a peakedness of 2.3 (Funke and Mansard, 1980). Zero crossing analysis and spectral analysis were used to analyze the wave records.

A movable carriage with an array of five capacitance wire wave probes was used to measure the wave heights over the full beach profile. The actual shape of the wooden profile was measured using a manual profiler a few days after filling the flume with water. The standard deviation for the water depth over the horizontal section was found to be 3 mm. For each test the wave statistics H_{rms}, H_s, H_{max}, and H_{mo} were determined as a function of distance along the profile. Stable wave heights for each of these wave statistics were deduced from these wave height profiles. Each irregular wave test was performed once with reflection and once without reflection.

Table 1 also shows 13 regular wave tests. Reflection was not tested for the regular waves because of instabilities in the waves. The scatter in the data for the regular wave tests was larger than that for the irregular wave tests. The regular wave tests were performed to compare the results with those obtained by Horikawa and Kuo (1966).

5. Determination of Γ

5.1. Tests without reflection

The coefficient Γ is required for the TDM and was determined for both H_{rms} and H_s. Figs. 4 and 5 depict as an example the results obtained for Test KA4, which had a significant deep water wave height of 7 cm and a water depth over the horizontal shelf of 10 cm. Similar results were obtained for the other 33 tests performed. Fig. 4 compares the values of the rms wave height obtained from wave statistics obtained by zero crossing analysis (labelled statistical) and the rms wave height obtained from a spectral analysis (labelled spectral). Although both definitions yielded identical results in deep water, the statistical value was consistently higher than the spectral value near the breaker. Nairn (1990), and Thompson and Vincent (1984) reached this same conclusion. All the tests performed showed that the values according to both definitions became nearly identical in the wave stabilizing zone

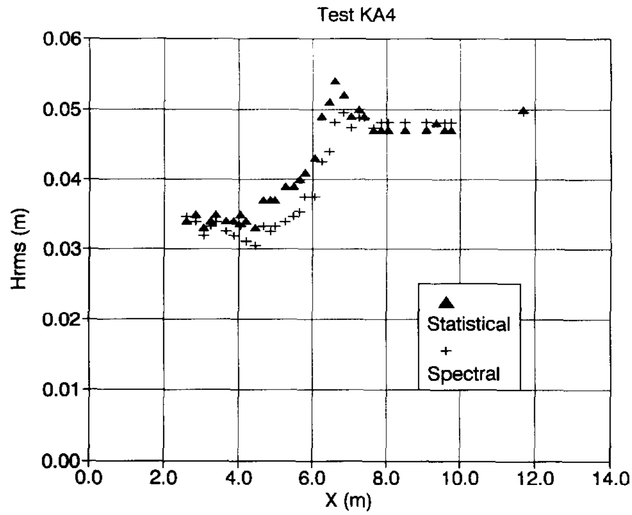

Fig. 4. Statistical and spectral wave height profiles.

over the horizontal shelf. For some tests both definitions were close throughout the wave decay zone.

Fig. 5 shows an example of the wave decay and stabilization of the wave statistics H_{rms}, H_s, and H_{max}. It can be seen that each of these wave statistics approaches its own stable wave height. Such figures show that Eq. (9) for regular waves can indeed be applied to any single wave height statistic using the appropriate coefficients, which need to be determined.

Fig. 6 plots the stable significant wave height against the still water level (SWL) depth over the horizontal shelf. A constant value of Γ_s would be represented by a straight line in

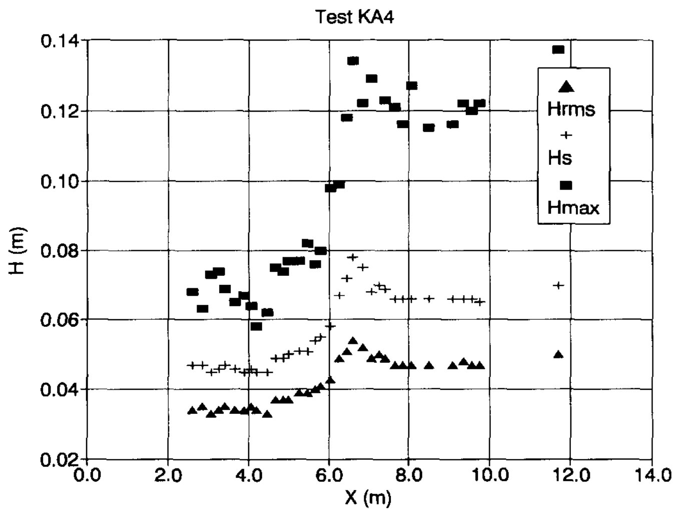

Fig. 5. Wave decay for different wave statistics.

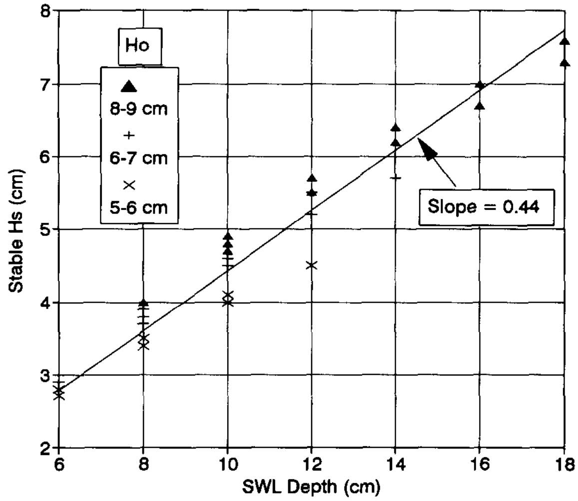

Fig. 6. Stable wave height as a function of SWL depth.

Fig. 6. The line shown on the figure is the best fit straight line; and has a slope of 0.44 ($r^2 = 0.92$). Fig. 7 gives a similar plot against the mean water level (MWL) depths. The MWL depths were obtained by adding the wave setup, calculated using a numerical model (Rakha and Kamphuis (1993)) to the SWL depth. The best fit in this case was a line with a slope of 0.43 ($r^2 = 0.95$). The legends in both Figs. 6 and 7 divide the data according to the deep water significant wave height. From the above figures an average value of $\Gamma_s = 0.43$ may be used. However, for the same water depth the larger incident wave heights produced larger stable wave heights implying some dependence on the deep water wave height. The data also shows that a nonlinear fit should give better results. These effects are shown later

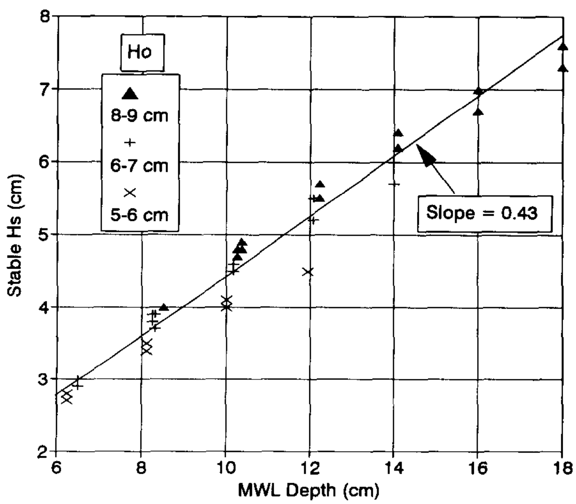

Fig. 7. Stable wave height as a function of MWL depth.

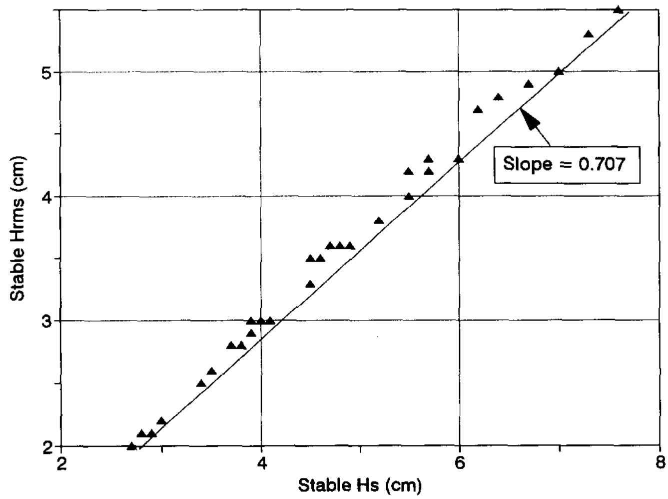

Fig. 8. rms stable wave height as a function of significant wave height.

on, to be a result of the dependency of Γ on the breaker wave steepness. Hardy et al. (1990) found that the value of Γ for the characteristic wave height was 0.4 on an offshore coral reef. Figures similar to Figs. 6 and 7 were obtained for the rms wave height, suggesting an average value of $\Gamma_{rms} = 0.32$.

Fig. 8 relates the statistical stable wave heights H_{rms} and H_s. From Fig. 8 it can be seen that the assumption that $H_{rms} = H_s/\sqrt{2}$ is not a bad assumption even in the wave stabilization zone. The best fit was given by $H_{rms} = 0.74H_s$ ($r^2 = 0.99$). The best fit for the maximum stable wave height H_{max} was given by $H_{max} = 1.49H_s$ ($r^2 = 0.96$), which differs from the value obtained by assuming a Rayleigh distribution.

As mentioned previously, a distinction between the statistical and spectral definitions is necessary. Fig. 9 shows that the characteristic wave height H_{mo}, defined from the wave spectrum and the statistical wave height H_s defined from the statistical wave height distribution are nearly identical in the wave stabilizing region. The data includes both cases with and without reflection. The cases with reflection showed that H_{mo} was slightly higher than H_s. Fig. 9 implies that the same value of Γ may be used for both definitions.

Dimensional analysis shows that,

$$\Gamma = f\left(\gamma_b, \left(\frac{H}{L}\right)_b, m\right) \tag{15}$$

where, f is an unknown function, γ_b is the breaker index $(H/d)_b$, $(H/L)_b$ is the breaker wave steepness, and m is the beach slope before the horizontal shelf. The beach slope was constant for all the tests performed, and its effect was not studied.

Fig. 10 depicts the dependence of Γ on the breaker index, the legends separate the two wave periods tested. It shows that there is no clear dependence on the wave period. Since the wave length is primarily a function of the wave period and the water depth only, the use of either the breaker index or the breaker steepness should therefore suffice. The range of wave periods tested cannot define the wave period effects. More tests with a larger range

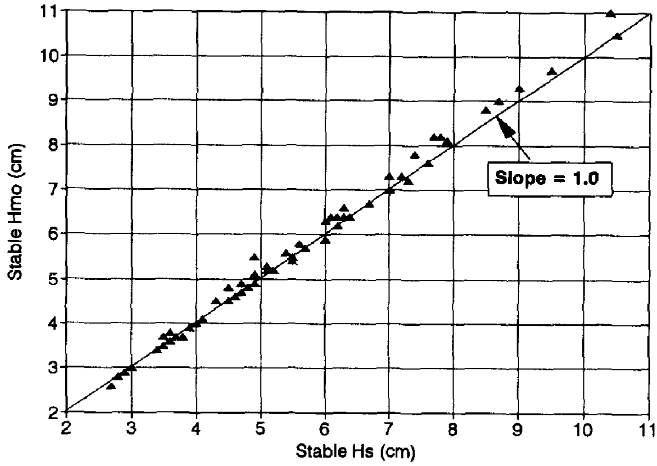

Fig. 9. Statistical and spectral stable wave heights.

of wave periods would be necessary. Figs. 11 and 12 show that less scatter than in Fig. 10 is obtained using the breaker wave steepness. That same observation was made by Kamphuis (1991) with respect to the breaker criterion.

Two best fit equations were obtained. The first is for the significant stable wave height,

$$\Gamma_s = 0.277 + 2.46\left(\frac{H_s}{L}\right)_b \tag{16}$$

with $r^2 = 0.78$ and the curve fit standard error $= 0.013$ for Γ_s and,

$$\Gamma_{rms} = 0.19 + 2.84\left(\frac{H_{rms}}{L}\right)_b \tag{17}$$

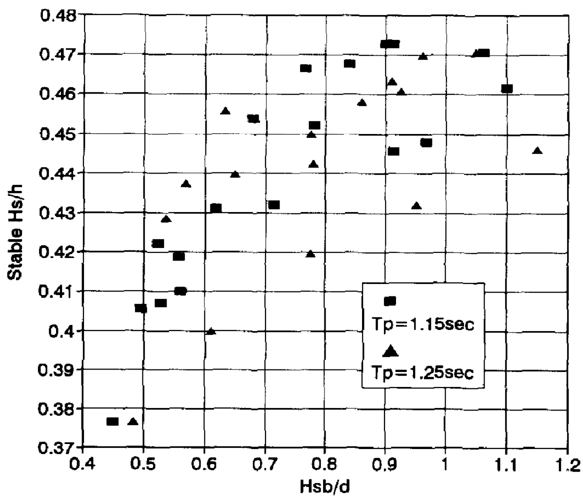

Fig. 10. Effect of breaker index and wave period on Γ.

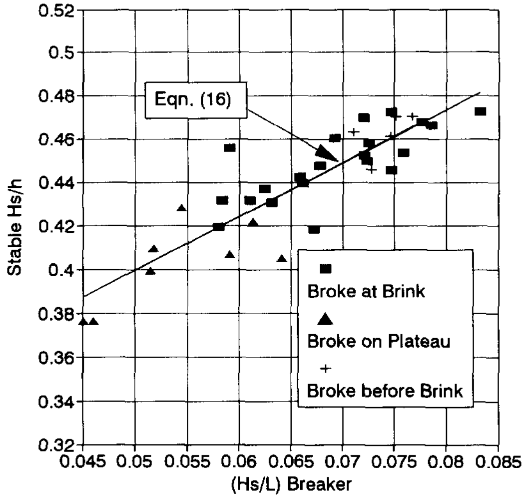

Fig. 11. Effect of breaker wave steepness on Γ_s.

with $r^2 = 0.78$ and the curve fit standard error = 0.011 for Γ_{rms}.

Larson's (1993) method was used to predict Γ_{rms} for the tests performed. Larson mentioned that for a monotonic beach, his model gave the same results as a Monte Carlo simulation. Fig. 13 shows that this method overpredicted the value of Γ_{rms} for larger wave steepness, which suggests that the Monte Carlo type of model will overpredict H_{rms} for these cases.

5.2. Tests with reflection

For tests with reflection, Figs. 14 and 15 provide sample results obtained for the total wave heights as measured for Test KA4. From Fig. 14 it can be observed that both the

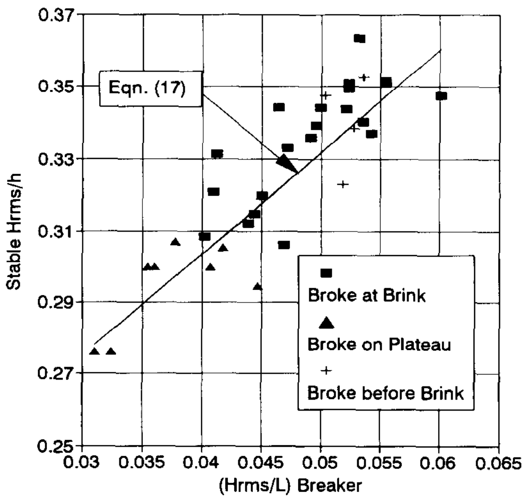

Fig. 12. Effect of breaker wave steepness on Γ_{rms}.

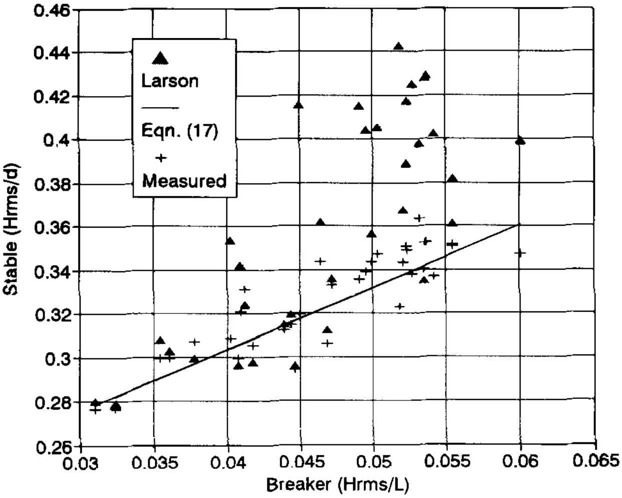

Fig. 13. Larson (1993) prediction for Γ_{rms}.

spectral and statistical definitions again yield similar results throughout the surf zone. Fig. 15 shows that each wave statistic again approaches its own stable wave height. The scatter in the maximum wave height was however observed to be larger for most of the tests with reflection, due to phase effects.

Fig. 16 relates the rms and significant stable total wave heights. The assumption that $H_{rms} = H_s/\sqrt{2}$ is shown to be reasonable; the best fit line gave a slope of 0.72.

Fig. 17 compares the H_{rms} stable wave height definition for cases with and without reflection. A best fit gave a slope of 1.31 ($r^2 = 0.98$). The results for the stable significant

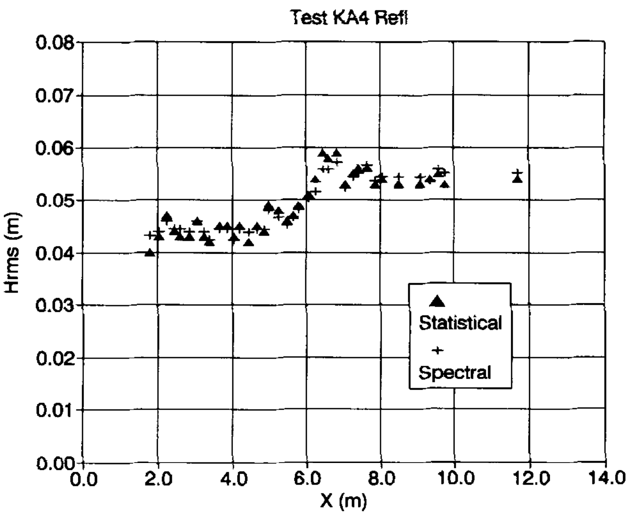

Fig. 14. Statistical and spectral wave height profiles (with reflection).

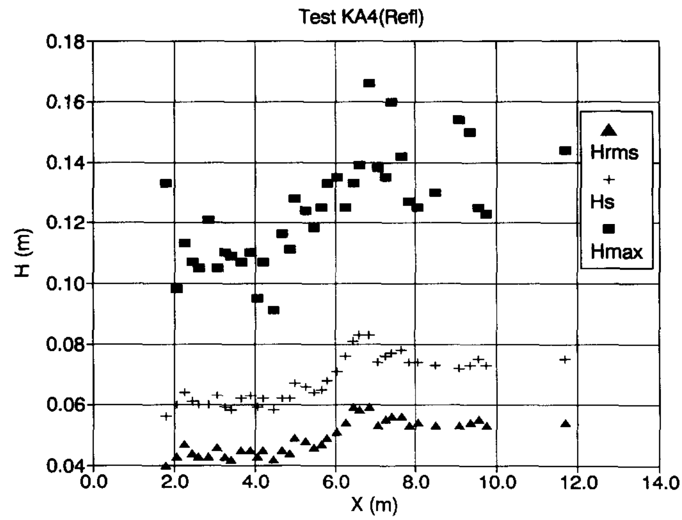

Fig. 15. Wave decay for different wave statistics (with reflection).

wave height gave a best fit with a slope of 1.34 ($r^2 = 0.98$). Finally, the stable characteristic wave heights for the cases with and without reflection gave a slope of 1.39 (r^2 of 0.98).

Substituting the commonly accepted value of $K_r = 0.9$ into Eq. (13) produces:

$$H_t = 1.34 H_i \tag{18}$$

which is close to the best fit obtained from the tests and thus the reflected wave does not affect the incident stable wave height. The assumption by Jones (1975) that the reflected wave does not lose energy due to the breaking process has also been confirmed. Also the

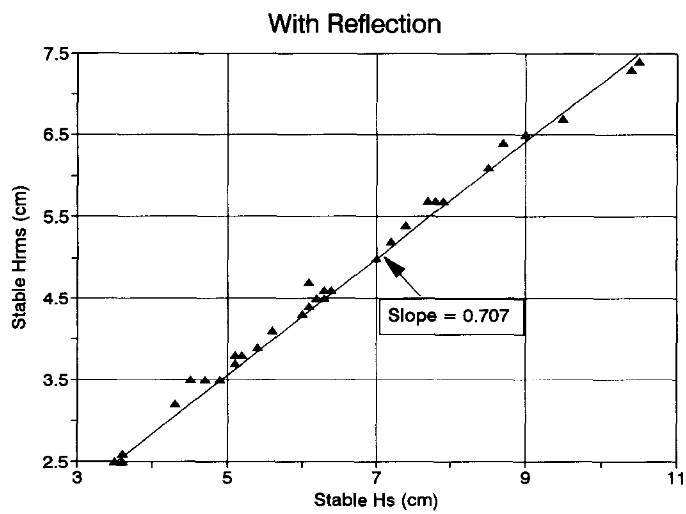

Fig. 16. rms stable wave height as a function of significant wave height (with reflection).

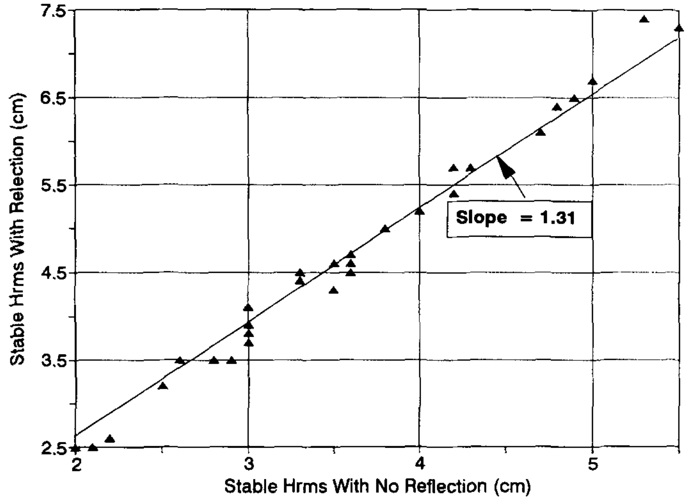

Fig. 17. Stable H_{rms} with reflection.

total wave height can be obtained by summing the energies of both the reflected and incident waves. The above conclusions are verified later by including them into a wave transformation model which predicted the wave heights well.

The above analysis was not performed for H_{max}, because Eq. (11) cannot be applied to individual wave heights in the wave record. The scatter in the results for H_{max} with reflection was larger than for other wave statistics because of nodal and antinodal points in the H_{max} profile, indicating phase effects. The actual value of H_{max} at each location is the maximum value of H within the wave cycle obtained by adding the local instantaneous reflected and incident waves. The incident wave that generated the reflected wave is different from the

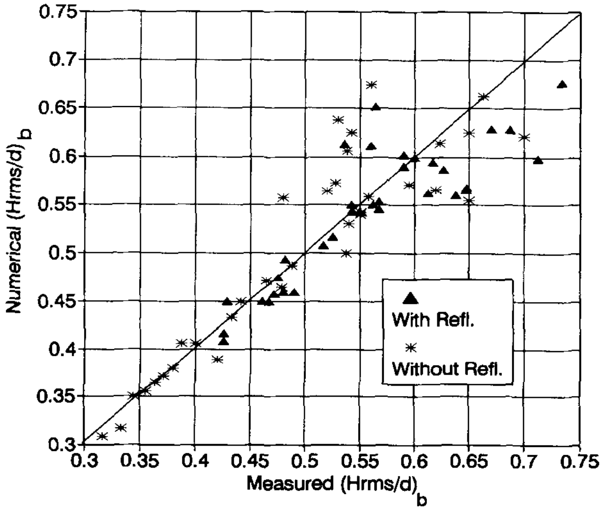

Fig. 18. Breaker criterion for all tests.

incident wave added to the reflected wave, thus the analysis of such a wave statistic would require a detailed Boussinesq type wave model. If the stable H_{max} is regarded as that value obtained for a smooth curve averaging all the individual points then the data obtained for H_{max} describes some trends. A graph of this stable H_{max} vs. H_s gave a best fit line with a slope of 1.7. Comparison of the H_{max} stable wave height definition for cases with and without reflection (similar to Fig. 17) gave a best fit line with a slope of 1.55. This value is less than the highest possible value for individual waves which would be close to 1.9, and greater than the values 1.31 and 1.34 obtained for the rms and significant wave statistics.

6. Breaker criterion

As mentioned earlier Eq. (14) was used together with the assumption $H_{rms} = \sqrt{2}H_s$ to determine the breaking criteria for H_{rms}, using the total wave height. Fig. 18 shows that Eq. (14) can be applied to the total wave height for the cases with reflection. The larger deviations were observed for the cases where the waves broke on the 1 : 10 slope. These deviations resulted from the inaccurate determination of the breaker location, because the distance between the wave probes was 20 cm while the numerical results provide the breaker location to the closest 5 cm.

7. Wave spectra

Fig. 19 shows the wave spectra at four distances from the baseline. The position $X = 6.6$ represents the brink position, and $X = 4.05$ represents the location where the wave is stable. Figs. 19a and 19c show that the peak period of the wave spectra decreases slightly as the waves decay. Hotta and Mizuguchi (1980) reported this same observation for field data. Some transfer of energy from the peak to the higher and lower frequencies was also observed, which is consistent with the findings of Smith and Hughes (1993).

Figs. 19b and 19d provide the wave spectra for tests KA4 and KA6 with reflection included. The wave spectra for these cases are similar to the corresponding tests without reflection, but the spectra without reflection were smoother.

8. Comparison with numerical model

The Γ coefficient in the TDM was calibrated above using the experimental results. Both models must now be compared with the tests to determine the value of K in case of the TDM and verify the FDM. Linear wave theory was used in both models referred to as LTDM and LFDM.

The models predicted the decay of the corresponding H_{rms} for Test KA6 well as shown in Fig. 20, where Eq. (17) was used in the LTDM. The value of $K = 0.15$ was used for all the tests and was found to fit the data well. For some of the tests, where the spectral definition was lower than the statistical definition, the LFDM overpredicted the wave height just after the breaker. The effect of reflection was also predicted using both proposed models as shown

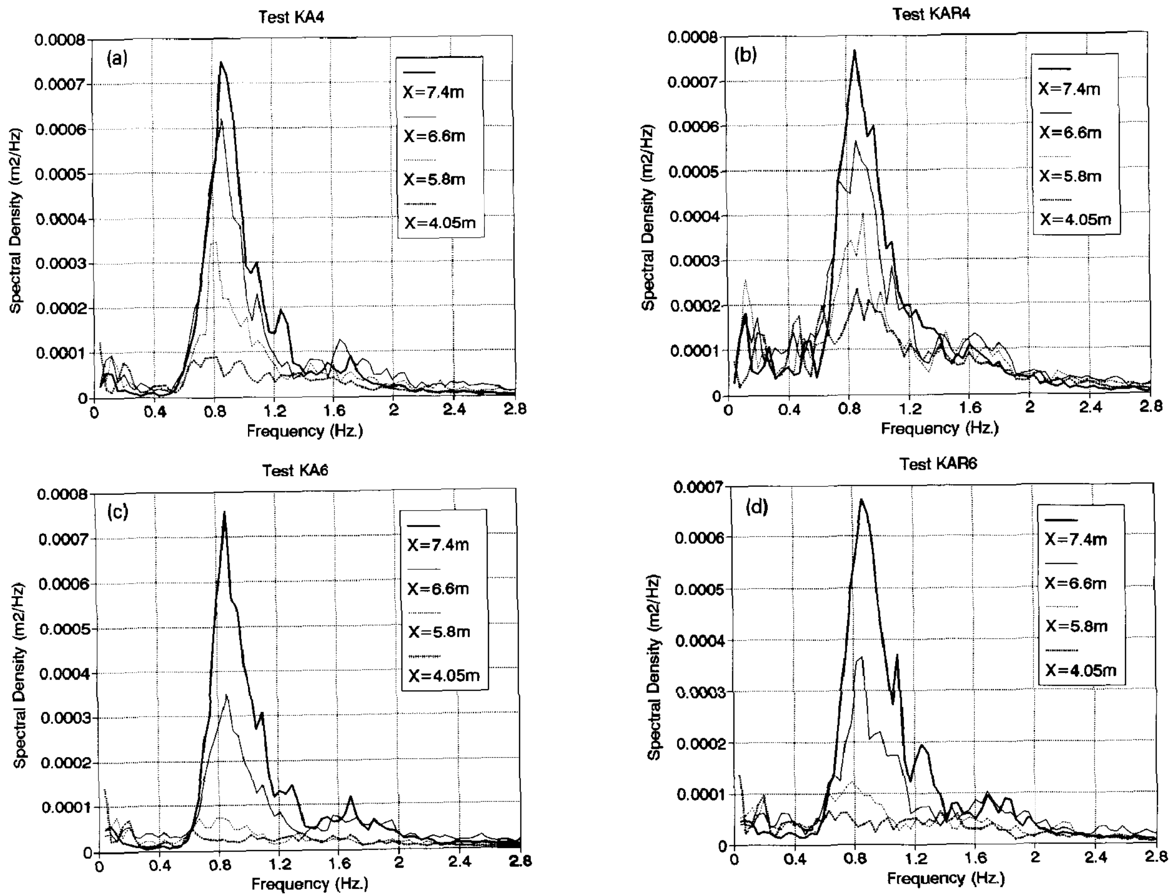

Fig. 19. (a) Wave spectra for Test KA4. (b) Wave spectra for Test KA4 (with reflection). (c) Wave spectra for Test KA6. (d) Wave spectra for Test KA6 (with reflection).

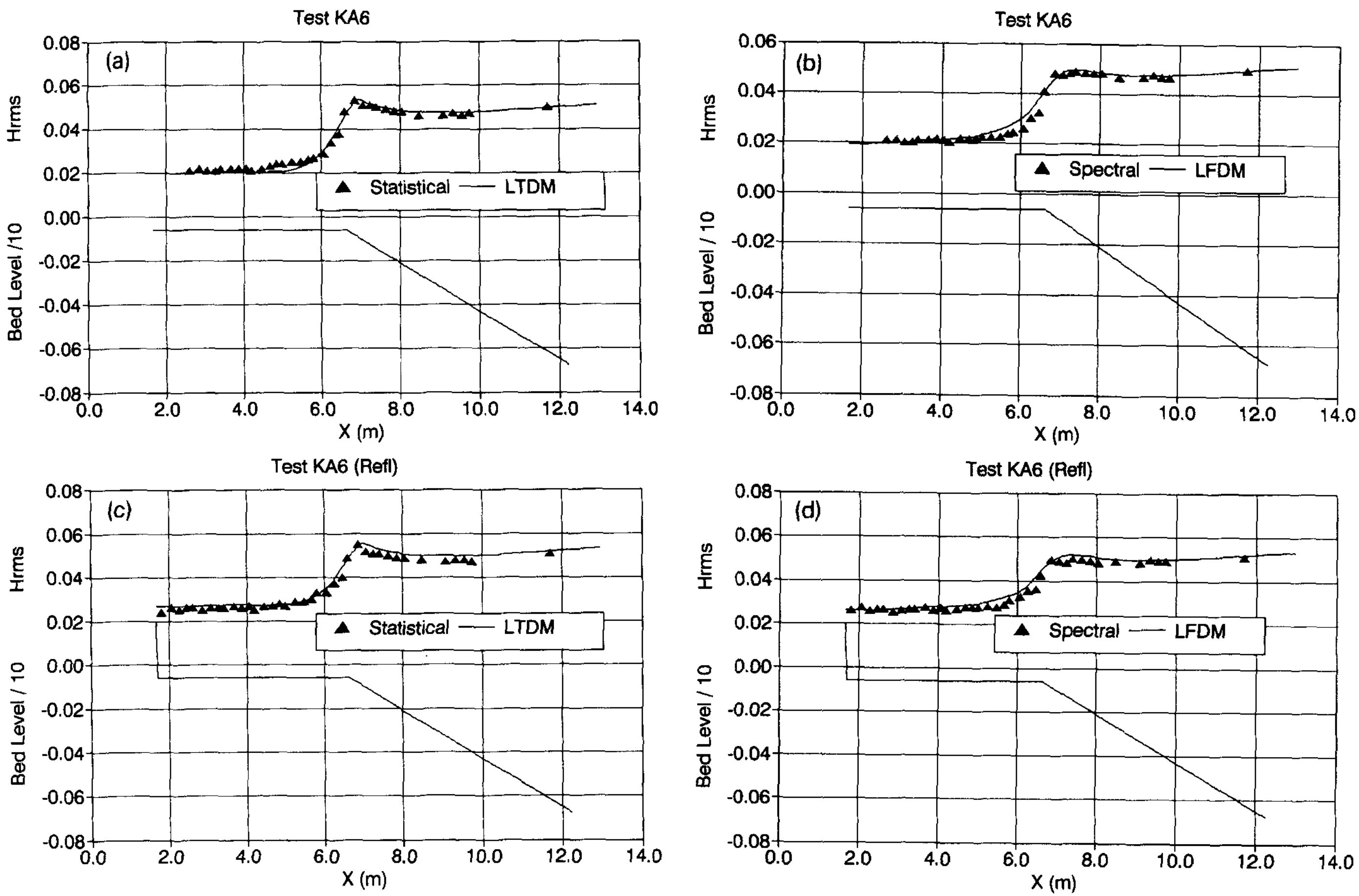

Fig. 20. (a) LTDM for Test KA6 without reflection. (b) LFDM for Test KA6 without reflection. (c) LTDM for Test KA6 with reflection. (d) LFDM for Test KA6 with reflection.

Table 2
Goodness of fit summary

Test	LTDM	LFDM
KA6	0.034	0.034
KAR6	0.027	0.027
Average of all tests	0.038	0.035
Standard deviation of error	0.012	0.01
Maximum error	0.084	0.078
Minimum error	0.02	0.017

in Figs. 20c and 20d. The results obtained for the rest of the tests are presented in Rakha (1995). Visually, both the TDM and the FDM have the same accuracy. Table 2 quantifies the errors for the tests performed. The measure of fit used is the standard deviation of the error normalized by the incident deep water wave height. This same measure was used by Kamphuis (1994),

$$e=\frac{\sqrt{\Sigma(H_{\mathrm{cal}}-H_{\mathrm{meas}})^2/N}}{H_{\mathrm{i}}} \tag{19}$$

Table 2 shows that the LFDM performed slightly better than the LTDM. The difference between both models was found to be insignificant for a confidence limit of 95%. Rakha and Kamphuis (1994) compared visually both the LTDM and the LFDM against 2D and 3D tests on fixed and sand beaches. The results for the 2D tests were similar but for the 3D tests with higher reflection, the LTDM predicted the wave heights better than the LFDM.

9. Summary

The stable wave height coefficient Γ for H_{rms} and H_{s} was calibrated against stable wave height tests on a shelf beach with irregular waves. Γ was found to depend on the breaker wave steepness. The tests were performed for a 1 : 10 slope followed by a horizontal shelf beach. The peak periods tested were 1.15 and 1.25 seconds. More tests with a larger range of periods and slopes would extend the proposed equations.

The wave height definition obtained from a statistical analysis of the wave heights differs from that obtained by a spectral analysis. The TDM was developed for the statistical wave definition, and the FDM for the spectral wave definition.

Both the TDM and the FDM were compared with 68 two dimensional hydraulic model tests. Both models predicted the wave decay of their corresponding wave statistics well. For some cases the FDM overpredicted the wave heights just after the breaker location.

The effect of wave reflection was included in both models, using a mirror image technique. The reflected wave did not lose energy through breaking, nor did it affect the energy dissipation for the incident wave. A reflection coefficient of 0.9 gave good results for a vertical seawall.

The Kamphuis (1991) breaker criterion predicts the breaker location for the total wave height well.

The wave spectra showed a transfer of energy to the higher and lower frequencies as the waves stabilized.

10. Notation

C_g = wave group velocity;
D = wave energy dissipation rate;
E = wave energy density;
E_{st} = stable wave energy density;
g = acceleration of gravity;
h = water depth to MWL;
H_i = incident wave height;
H_m = maximum wave height for depth h;
H_{mo} = characteristic wave height;
H_r = reflected wave height;
H_{rms} = root mean square wave height;
H_s = significant wave height;
H_{sb} = significant breaking wave height;
H_{st} = stable wave height;
H_t = total wave height;
k = wave number;
L_{pb} = wave length for peak period at breaker;
m = beach slope;
Q = fraction of waves breaking;
T_p = peak period;
X = offshore distance from baseline;
γ = empirical constant;
γ_b = breaker index;
Γ = empirical constant for stable wave;
K = wave decay rate empirical constant;
ρ = fluid density.

Acknowledgements

This study was carried out under the Strategic Grants Program of the Natural Sciences and Engineering Research Council (NSERC) of Canada. The first author also received a scholarship from Queen's University of Canada, and a study leave from Cairo University of Egypt.

References

Battjes, J.A. and Janssen, J.P.F.M., 1978. Energy loss and set-up due to breaking of random waves. In: Proc. 16th Int. Conf. Coastal Eng., Hamburg. ASCE, New York, Vol. 1, pp. 569–589.

Battjes, J.A. and Stive, M.J.F., 1984. Calibration and verification of a dissipation model for random breaking waves. In: Proc. 19th Int. Conf. Coastal Eng., Houston, TX. ASCE, New York, Vol. 1, pp. 649–660.

Battjes, J.A. and Stive, M.J.F., 1985. Calibration and verification of a dissipation model for random breaking waves. J. Geophys. Res., 90(c5): 9159–9167.

Briand, M.H.G., 1990. A detailed quasi 3-D numerical model for sediment processes in the surf zone. Ph.D. thesis, Dept. of Civil Eng., Queen's University, Kingston, Canada, Sept. 1990, 304 pp.

Carr, J.H., 1952. "Wave Protection Aspects of Harbour Design". California Institute of Technology, Hydrodynamics Laboratory Report No. E-11.

Dally, W.R., Dean, R.G. and Dalrymple, R.A., 1984. A model for breaker decay on beaches. In: Proc. 19th Int. Conf. Coastal Eng., Houston, TX. ASCE, New York, Vol. 1, pp. 82–98.

Dally, W.R. and Dean, R.G., 1986. Transformation of random breaking waves on surf beat. In: Proc. 20th Int. Conf. Coastal Eng., Taipei. ASCE, New York, Vol. 1, pp. 109–123.

Funke, E.R. and Mansard, E.P.D., 1980. On the synthesis of realistic sea states. In: Proc. 17th Int. Conf. Coastal Eng., Sydney. ASCE, New York, Vol. 3, pp. 2974–2991.

Goda, Y., 1976. Estimation of incident and reflected waves in random wave experiments. In: Proc. 15th Int. Conf. Coastal Eng., Honolulu, HI. ASCE, New York, Vol. 1, pp. 828–845.

Goda, Y., 1985. Random Seas and Design of Maritime Structures. University of Tokyo Press, 323 pp.

Hardy, T.A., Young, I.R., Nelson, R.C. and Gourlay, M.R., 1990. Wave attenuation on an offshore coral reef. In: Proc. 22nd Int. Conf. Coastal Eng., Delft. ASCE, New York, Vol. 1, pp. 330–344.

Horikawa, K. and Kuo, C.T., 1966. A study on wave transformation inside surf zone. In: Proc. 10th Int. Conf. Coastal Eng., Tokyo. ASCE, New York, Vol. 1, pp. 217–233.

Hotta, S. and Mizuguchi, M., 1980. A field study if waves in the surfzone. Coastal Eng. Jpn., 23: 79–89.

Ippen, A.T., 1966. Estuary and Coastline Hydrodynamics. McGraw-Hill, New York.

Johnson, H., 1990. Interactions between waves and currents in the surf zone. Ph.D. thesis, Dept. of Civil Eng., Queen's University, Kingston, 322 pp.

Jones, D.F., 1975. The effect of vertical seawalls on longshore currents. Ph.D. thesis, Dept. of Coastal and Oceanographic Eng., University of Florida, Gainesville, FL, 188 pp.

Kamphuis, J.W., 1991. Incipient wave breaking. Coastal Eng., 15: 185–203.

Kamphuis, J.W., 1994. Wave heights from deep water through the breaking zone. J. Waterw. Port Coastal Ocean Eng. ASCE, 120(4): 347–367.

Kondo, K., Akama, M. and Isobe, M., 1986. Measurement of reflection coefficient. In: Proc. 20th Int. Conf. Coastal Eng., Taipei. ASCE, New York, Vol. 2, pp. 1987–2001.

Larson, M., 1993. Model for decay of irregular waves in the surf zone. Report 3167, Dept. of Water Resources Eng., Lund University, Sweden, 50 pp.

LeMéhauté, B., 1962. On the nonsaturated breaker theory and the wave run-up. In: Proc. 8th Int. Conf. Coastal Eng., Mexico. ASCE, New York, pp. 77–92.

Longuet-Higgins, M.S., 1983. On the joint distribution of wave periods and amplitudes in a random wave field. In: Proc. R. Soc. London, A389: 241–258.

Nairn, R.B., 1990. Prediction of cross-shore sediment transport and beach profile evolution. Ph.D. Thesis, Dept. of Civil Eng., University of London, 294 pp.

Rakha, K.A. and Kamphuis, J.W., 1993. Wave setup near a seawall: experiments and a numerical model. In: Waves 93. ASCE, New York, pp. 835–848.

Rakha, K.A. and Kamphuis, J.W., 1994. Wave transformation in the vicinity of a seawall. In: International Symposium Waves — Physical and Numerical Modelling, Vancouver, pp. 1011–1020.

Rakha, K.A., 1995. Seawalls; a numerical and physical study. Ph.D. thesis, Dept. of Civil Eng., Queen's University, Kingston.

Schäffer, H.A., Madsen, P.A. and Deigaard, R., 1993. A Boussinesq model for waves breaking in shallow water. Coastal Eng., 20: 185–202.

Silvester, R., 1974. Coastal Engineering, Vol. 1. Elsevier, Amsterdam, pp. 320–321.

Singamsetti, S.R. and Wind, H.G., 1982. Breaking waves. Characteristics of shoaling and breaking periodic waves normally incident to plane beaches of constant slope. Delft Hydraulic Laboratory Report No. M1371.

Smith, E.R. and Hughes, S.A., 1993. Shoaling of wave spectra in front of reflective structures. In: Waves 93. ASCE, New York, pp. 642–655.

Thompson, E.F. and Vincent, C.L., 1984. Shallow water wave height parameters. J. Waterw. Port Coastal Ocean Eng., 110(2): 293–298.

Thornton, E.B. and Guza, R.T., 1983. Transformation of wave height distribution. J. Geophys. Res., 88(C10): 5925–5938.
Weggel, R.J., 1972. Maximum breaker height. J. Waterw. Port Coastal Ocean Eng. ASCE, WW4: 529–548.